Pharmacogn. Res., 2025; 17(2):1-11.
https://www.phcogres.com

Original Article

Green Synthesis of Silver Nanoparticles from *Secamone emetica*: Characterization and Assessment of Antioxidant, Anti-Diabetic and Anti-Cancer Activities against MCF-7 Breast Cancer Cells

S. Shalini*, N. Sudeepthi, DH. Geetha, R. Jayashre

Department of Botany, Vellalar College for Women (Autonomous), Erode, Tamil Nadu, INDIA.

ABSTRACT

Background: Green-synthesized nanoparticles offer eco-friendly advantages over physical and chemical methods, utilizing plant extracts as natural capping, reducing and stabilizing agents. While *Secamone emetica* is renowned for its traditional medicinal applications, its potential in green nanoparticle synthesis remains unexplored, offering a promising avenue for research. **Objectives:** This study aimed to synthesize silver Nanoparticles (AgNPs) using aqueous leaf and stem extracts of *Secamone emetica* and evaluate their antioxidant, anti-diabetic and anti-cancer properties. **Materials and Methods:** The aqueous extracts of *S. emetica* Leaf (SL) and Stem (SS) were used for the green synthesis of AgNPs. The bio-reduction of silver ions by these extracts was validated through UV-visible spectroscopy, X-ray Diffraction (XRD), Scanning Electron Microscopy (SEM) and Fourier-Transform Infrared Spectroscopy (FTIR). Antioxidant activities were evaluated using DPPH+ and $ABTS^{\cdot}+$ radical scavenging assays. The anti-diabetic potential was evaluated through α-amylase and α-glucosidase inhibition assays. Cytotoxic effects on MCF-7 breast cancer cell lines were assessed at 100 µg/mL concentration. **Results:** SL-AgNPs exhibited higher antioxidant activity compared to SS-AgNPs in both DPPH+ and $ABTS^{\cdot}+$ assays. In anti-diabetic assays, SL-AgNPs demonstrated 70.1% α-amylase inhibition and 68.4% α-glucosidase inhibition, outperforming SS-AgNPs, which showed 59.3% and 57.6% inhibition, respectively. In the anti-cancer assay, SL-AgNPs exhibited a cytotoxicity of 62.5% against MCF-7 cells, whereas SS-AgNPs showed 50.8% inhibition. **Conclusion:** These findings highlight the potential of green-synthesized SL-AgNPs and SS-AgNPs as effective antioxidant, anti-diabetic and anti-cancer agents.

Keywords: *Secamone emetica*, Silver nanoparticles, Antioxidant activity, Anti-diabetic, Anti-cancer, cytotoxicity.

Correspondence:
Ms. S.Shalini
Ph.D. Research Scholar, PG and Research Department of Botany, Vellalar College for Women (Autonomous), Erode-638012, Tamil Nadu, INDIA.
Email: sshalinishalu128@gmail.com

Received: 12-11-2024;
Revised: 06-01-2025;
Accepted: 25-02-2025.

INTRODUCTION

Nanotechnology is a dynamic and rapidly evolving field with wide applications in science and technology.[1] Nanoparticle-based therapies provide targeted delivery, reducing the demand for high doses and minimizing side effects.[2] Traditional methods such as physical, thermal, hydrothermal and chemical approaches are expensive, hazardous and dependent on toxic chemicals. Consequently, attention has been directed towards green synthesis, an eco-friendly alternative that utilizes biological resources for the efficient formulation of Nanoparticles (NP). This eco-friendly approach emphasizes the practice of renewable and environmentally benign compounds as reducing and capping agents.[3]

The oxidation-reduction properties of plant extracts, which include bioactive compounds such as alkaloids, polyphenols, terpenoids, sugars and proteins, play a critical role in reducing and stabilizing metal ions. These compounds also act as topping agents, facilitating nanoparticle production.[4] Among metallic nanoparticles, silver Nanoparticles (AgNPs) are less toxic to mammalian cells than other types. Their modest size enables them to penetrate through cell membranes effortlessly, making them potent antimicrobial agents.[2]

In the view of Bedlovikova *et al.*, the coating of flavonoids, phenolics and terpenoids on the top of AgNPs, enables their function as singlet oxygen quenchers, hydrogen donors and reductants, thereby enhancing their antioxidant capacity compared to plant extract.[5] Additionally, green-synthesized

DOI: 10.5530/pres.20252064

silver nanoparticles have demonstrated promising potential in managing and balancing metabolic and health disorders, including diabetes mellitus, arthritis, neurodegenerative diseases and various cancers, by acting as antioxidant agents.[6] In this context, plants from the family Apocynaceae have been treasured for potent supplies of multiple alkaloids and their endorsed medicinal properties.[7,8]

Secamone emetica an endemic plant of the Apocynaceae family has been conventionally used in folk medicine to treat headaches, leucorrhoea, fever and dysentery. Notably, the Paliyan tribes of the Sirumalai Hills have also utilized this plant to treat nervous disorders.[9,10] Phytochemical studies on *S. emetica* revealed the presence of metabolites like flavonoids, alkaloids, phenols, terpenoids, tannins and glycosides.[11] While milky latex contains several secondary metabolites rich in hydrocarbon content.[12] Sini *et al.*, (2010) reported the antioxidant capacities of the plant's fruits and leaves.[13] In spite of its notable potential, research on the green synthesis of nanoparticles from *Secamone emetica* and their biological activities remains surprisingly unexplored. Thus, this work creates new ground by being the first to showcase green-synthesized nanoparticles from *Secamone emetica* and highlights their remarkable potential in antioxidant, anti-diabetic and anticancer activities.

MATERIALS AND METHODS

Collection and authentication of Plant

Plant materials were gathered from Palamalai (11°45´latitude and 77°44´longitude, at an altitude of 1050-1100M above Mean Sea Level), Mettur, Erode District, Tamil Nadu, India. The specimen was botanically identified and authenticated at the Botanical Survey of India (BSI), Southern Circle, Coimbatore, Tamil Nadu, India with the voucher specimen number BSI/SRC/5/23/2022/Tech.528.

Preparation of extract

The leaves and stem of *S. emetica* were separated and rinsed softly with tap water to clear adhering dust soil particles and surface sterilized with 0.1% Sodium Hypochlorite (NaOCl) for 2 min, afterwards washed three times with distilled water and shade dried at ambient room temperature. The dried materials were powdered using an electronic blender. 25 g of leaf powder was combined with 250 mL of distilled water and heated at 80°C for 3 hr with continuous stirring. Subsequently, the mixture was strained with Whatman filter paper no. 1 and the resulting extract was kept at 4°C for further analysis.

Preliminary phytochemical analysis

A preliminary phytochemical assessment was carried out to identify various phytoconstituents such as alkaloids, flavonoids, phenols, tannins, terpenoids, steroids, coumarins, saponins, quinine, anthraquinone and glycosides in the leaves and stem aqueous extract of *Secamone emetica* using standard procedures.[14-17]

Green Synthesis of Silver Nanoparticles (AgNPs)

The previously prepared aqueous leaf and stem extract of *S. emetica* was used for the green synthesis of silver nanoparticles. A total of 10 mL of extract was combined with 90 mL of 1 mM silver nitrate solution, which was then heated at 80°C for 3 hr with continuous stirring. The color change from yellow to dark brown indicates the development of AgNPs. The green-synthesized nanoparticles were then separated by centrifugation at 15,000 rpm for 20 min. The resulting pellet was dried and stored at 4°C until further analysis.[18]

Characterization of Silver Nanoparticles (AgNPs)

UV-vis Spectroscopic Measurements

The plasmon-resonance properties of the developed Silver Nanoparticles (AgNPs) were examined using UV-vis spectroscopy. The transformation of silver nitrate with *S. emetica* extract was monitored using an HMG Labtech SPECTR Ostar Nano spectrophotometer. Measurements were conducted over a wavelength range of 220-700 nm with a resolution of 1 nm.

XRD Analysis

The crystalline nature of AgNPs was evaluated by X-ray Diffraction (XRD) investigation. Fine powdered SL-AgNPs and SS-AgNPs were drop-coated on an XRD grid to make a thin film. The diffraction patterns were noted using a Rigaku-Ultima IV diffractometer in Cu-Kα radiation (λ=0.154178 nm) at ambient temperature in a 2θ range of 7 to 80°, at a scan rate of 0.2°/min. with a time constant of 2 s in 2 hr.

Scanning Electron Microscopy

SEM analysis was executed to examine the shape, size and surface area of the AgNPs. After 15 min of ultrasonication at room temperature, one drop of the sample was deposited onto the AgNP solutions. The glass slide was coated in gold after drying and it was then examined under an SEM (Zeiss Evo-MA 10, Germany).

Fourier Transform Infrared (FT-IR) Analysis

The functional group involved in the reduction and capping of AgNPs was analyzed using n FTIR spectrophotometer (PerkinElmer Spectrum Version 10.4.00, M/s PerkinElmer Co., Waltham, Massachusetts) via the KBr pellet method. The FTIR spectrophotometer operated within a scanning range of 4000-400 cm-1, with a spectral resolution of 1 cm-1.

Antioxidant Activity

DPPH⁺ Free Radical Scavenging Assay

The antioxidant ability of the aqueous leaf and stem extract was assessed using the DPPH radical scavenging method. Specifically, 100 µL of varying levels of SL-AgNPs and SS-AgNPs, along with the standard (ascorbic acid) at concentrations of 10, 20, 50, 75, 100 and 150 µg/mL, were mixed with 100 µL of DPPH (0.1 mM in 80% ethanol) and allowed to incubate in the dark at Room Temperature (RT) for 30 min. The absorbance of the resulting mixtures was quantified at 517 nm using a spectrophotometer, with 80% ethanol serving as the blank. The DPPH free radical scavenging activity percentage was estimated with the following formula:

% of DPPH radical scavenging ability =[(Abs of control × 100-Abs of sample)/Abs of control].

The IC_{50} values for both the extract and nanoparticles were obtained from the graph using the equation Y=mX and the linear regression coefficient.

ABTS$^{\bullet+}$ Free Radical Scavenging Assay

The ABTS radical scavenging activity of multiple concentrations of the SL-AgNPs and SS-AgNPs was determined using a standard protocol. A stock solution of ABTS was formulated by mixing 7 mM ABTS with 2.45 mM potassium persulfate, followed by incubation in the dark for 16 hr at room temperature. The working solution was then prepared by diluting the stock solution with methanol until an absorbance of approximately 0.85±0.20 at 734 nm was achieved. Subsequently, 20 µL of varying concentrations of SL-AgNPs and SS-AgNPs (10, 20, 50, 75, 100 and 150 µg/mL) were mixed with 180 µL of the ABTS test solution. After allowing the mixture to sit for 30 min at room temperature, the absorbance was measured at 734 nm using a BMG Labtech spectrophotometer, with ascorbic acid serving as the standard. The percentage of ABTS free radical scavenging activity was determined by the following formula:

% of ABTS radical scavenging =[(Abs of control × 100 − Abs of sample) /Abs of control] × 100.

In vitro Anti-Diabetic Assay

Inhibition assay for α-amylase activity

α-Amylase was pre-incubated with the extract at different concentrations (50-200 µg/mL) and the reaction was started by adding 0.5% starch solution as the substrate. The process was conducted for 5 min at 37°C and then stopped by adding 2 mL of DNS (3,5-dinitrosalicylic acid) reagent. The mixture was subjected to heating for 15 min at 100°C and then diluted with 10 mL of distilled water immersed in an ice bath.[19] The activity of α-amylase was calculated by measuring the absorbance at 540 nm. The IC_{50} value was determined as the concentration of the α-amylase inhibitor required to inhibit 50% of the enzyme's activity under these assay conditions.

Inhibition assay for α- glucosidase activity

α-Glucosidase (0.075 units) was combined with the extract at varying concentrations (50-200 µg/mL). The reaction was started by adding 3 mM p-Nitrophenyl Glucopyranoside (pNPG) as the substrate.[19] The mixture was maintained at 37°C for 30 min, after which the reaction was stopped by including 2 mL of Na_2CO_3. The α-glucosidase activity was assessed by measuring the release of p-nitrophenol from pNPG at 400 nm. The IC_{50} value was determined as the concentration of the α-glucosidase inhibitor required to inhibit 50% of the enzyme's activity under the assay conditions.

Cytotoxicity study on Cancer cell line by MTT assay (MCF-7 Cancer Cell line)

The MCF-7 Human breast cancer cell line was procured from NCCS, Pune, India. The cells were cultivated in DMEM low glucose media enriched with 10% FBS, along with 1% antibiotic-antimycotic solution, in an atmosphere of 5% CO_2 and 18-20% O_2 at 37°C in a CO_2 incubator. The cells were sub-cultured every 3 days.

For the experiment, 200 µL of cell suspension was brought into a 96-well plate at a cell density of 20,000 cells per well, with no test agent added. The cells were allowed to grow for approximately 24 hr. Appropriate concentrations of SL-AgNps and SS-AgNps (6.25, 12.5, 25, 50 and 100 µg/mL)) were then included and the plate was maintained at 37°C for 24 hr in a 5% CO_2 atmosphere.

Following the incubation period, the plates were taken out from the incubator, the spent media was discarded. MTT reagent was introduced to achieve a final concentration of 0.5 mg/mL in the complete volume. The plates were wrapped in aluminium foil to prevent light exposure and returned to the incubator for a 3 hr incubation.

After incubation, the MTT reagent was removed and 100 µL of solubilization solution (DMSO) was added. Mild agitation on a gyratory shaker was applied to facilitate dissolution. From time to time, pipetting up and down was essential to completely dissolve the MTT formazan crystals, particularly in dense cultures. The absorbance was then measured on a spectrophotometer or ELISA reader at a wavelength of 570 nm.[20,21]

The cell viability percentage was calculated using the formula:

% cell viability =[Mean absorbance of treated cells / Mean absorbance of untreated cells] x 100.

Statistical Analysis

The experiments were performed in triplicates and denoted as mean±standard deviation. For graphical representation, GraphPad Prism 10.3.1 (509) were used.

RESULTS AND DISCUSSION

This study explored the biosynthesis of *Secamone emetica* silver nanoparticles (Se-AgNPs) and evaluated the nanoparticles' anti-oxidant, anti-diabetic capacity using the aqueous of *S. emetica*.

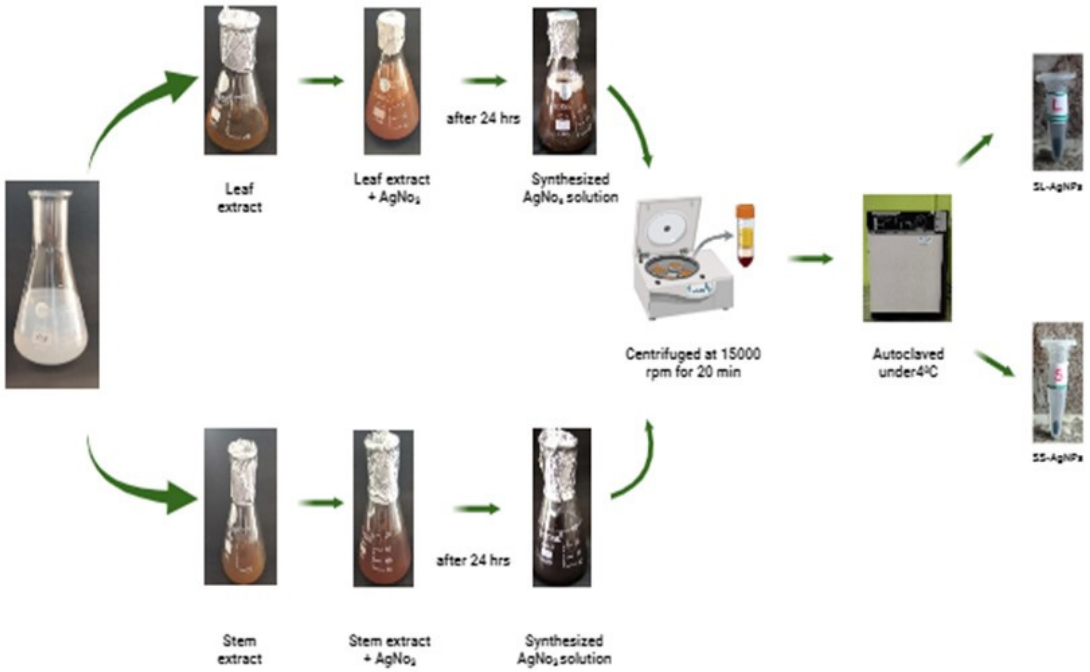

Figure 1: Schematic diagram illustrating the synthesis of silver nanoparticles using the leaf and stem extract of *Secamone emetica*.

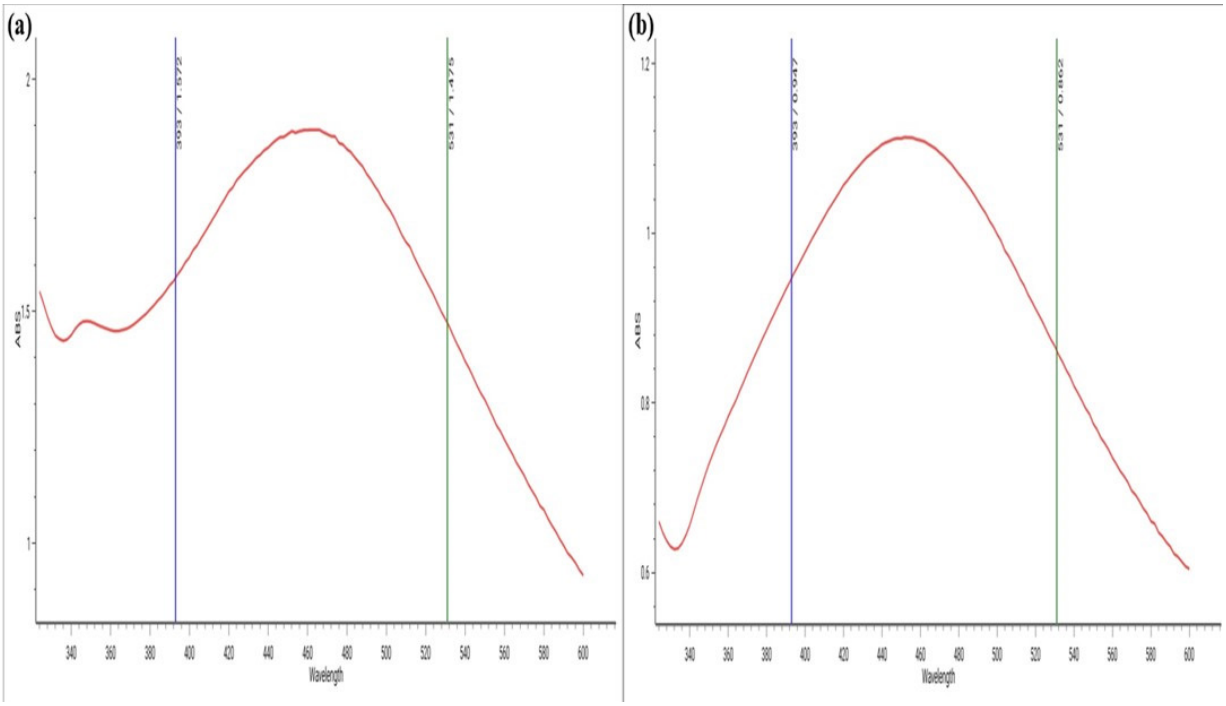

Figure 2: UV spectra of (a) SL-AgNPs and (b) SS-AgNPs.

Phytochemical Analysis

Various phytochemical compounds found in the aqueous extract of *S. emetica*, which contribute to the reduction and capping of silver nanoparticles, were qualitatively analyzed. Phytochemical screening showed that the leaf and stem extract of *S. emetica* contains notable phytoconstituents, as represented in Table 1. Our results exhibited slight variations from those described by Vaiyapuri *et al.*, (2015), particularly by the presence of tannins.[11] These phytoconstituents are accountable for reducing silver ions and acting as capping agents, preventing the aggregation of nanoparticles and enhancing their stability.[22]

Characterization of Se-AgNPs

After 24 hr of reaction time, the bio-reduction process of Ag^{+} to Ag^{0} by phytoconstituents in leaf and stem extracts of *S. emetica* was validated by the color variations from dark red to brown color, as show in Figure 1. A similar pattern of color changes was noted in the AgNPs from the leaf extract of *Ctenolepis garcini.*[23]

UV/visible Spectrum Analysis

The green synthesis of AgNps was confirmed by UV-vis spectroscopic analysis. The appearance of an absorbance peak around 420 nm in SL-AgNPs and 450 nm in SS-AgNPs specifies the formation of silver Nanoparticles (AgNPs) in the solution, attributed to the Surface Plasmon Resonance (SPR) of electrons existing on the nanoparticle surface,[24] as shown in Figures 2a and 2b. The observed peak values correspond with prior findings that reported an SPR peak at 415 nm for AgNPs using the *Ctenolepis garcini* plant extract[23] and an SPR peak at 440 nm for AgNPs from *Combretum indicum* extract.[25] Similarly, AgNps from *Trachyspermum ammi* and *Papaver somniferum* exhibited SPR vibrations at 430 nm.[26] The variations in peak values across studies may be directly aligned with the bio-reduction potential of the respective samples.

X-ray Diffraction (XRD) Analysis

The AgNPs were subjected to powder X-ray Diffraction (XRD) analysis for phase determination of the crystalline structure of nanoparticles. Examination of the graph for SL-AgNPs (Figure 3a) revealed strong peaks at 2θ values of 27.90°, 32.34°, 38.22°, 44.47°, 46.19°, 54.89°, 57.51°, 64.52°, 67.52°, 74.49°, 76.91°, 81.78° and 85.72°. Among these, six peaks at 38.22°, 44.47°, 64.52°, 76.91°, 81.78° and 85.72° at 2θ were matched with (111), (200), (220), (311), (222), (400) reflections respectively, indicating the face-cantered cubic (FCC) structure of metallic silver.

Similarly, for SS-AgNps (Figure 3b) strong peaks were observed at 2θ values of 27.85°, 32.203°, 38.105°, 44.293°, 46.217°, 54.823°, 57.475°, 64.475°, 64.417°, 77.417° and 81.693°. Among these, 2θ values at 38.105°, 44.293°, 64.475°,64.417°, 77.417° and 81.693°

Table 1:Preliminary Phytochemical screening of aqueous extracts of stem of *Secamone emetica*.

Phytoconstituents	Aqueous leaf extract	Aqueous Stem extract
Tannins	+	+
Flavonoids	-	-
Alkaloids	+	+
Triterpenoids	-	-
Phenols	+	+
Saponins	-	-

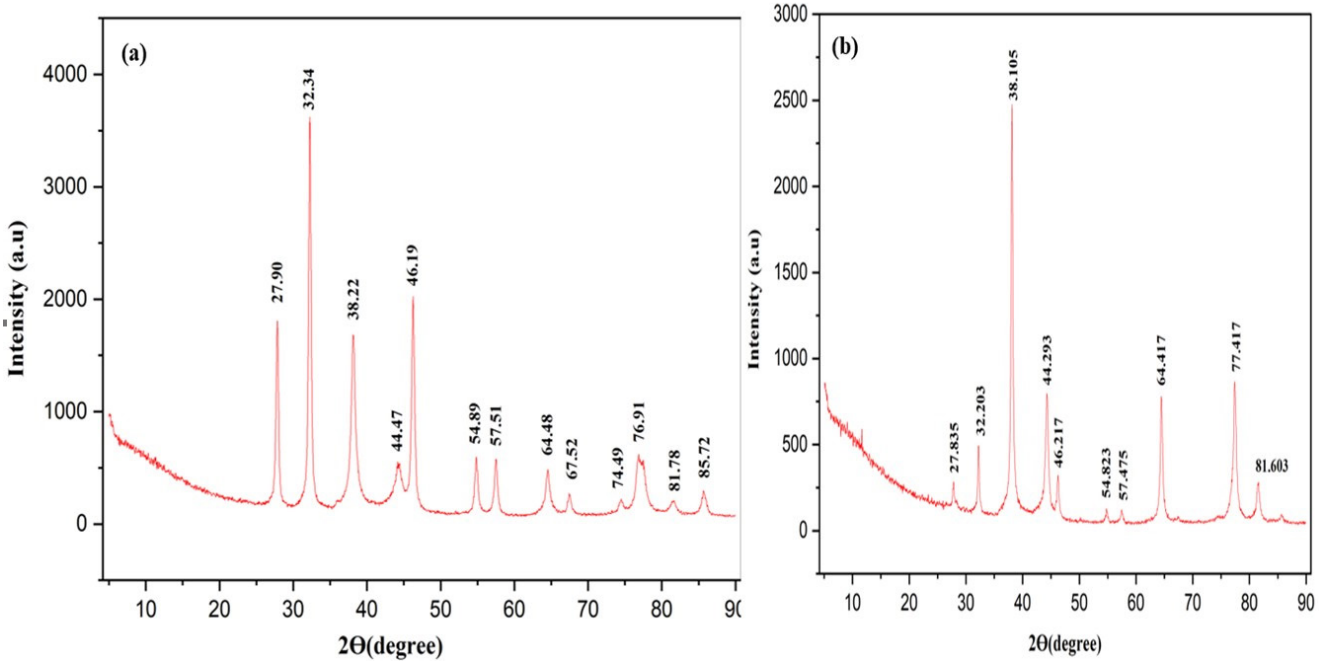

Figure 3: XRD graph patterns of (a) SL-AgNPs and (b) SS-AgNPs.

correspond to the (111), (200), (220), (311) and (222) reflections respectively, confirming FCC structure of metallic silver.

These distinctive peaks in both SL-AgNPs and SS-AgNPs confirm that the synthesized nanoparticles are composed of pure crystalline silver, as validated by assessment with JCPDS file no. 04-0783. Additionally, AgNPs synthesized using *Ctenolepis garcini, Eruca sativa* and *Spinacia oleracea* extracts exhibited nearly similar strong peaks at 27.94º, 32.36º, 46.36º and 56.28º.[23,27]

Additional, yet unassigned peaks were detected indicating that the crystallization of bio-organic phase occurs on the top of the silver nanoparticles.[28,29] The sharp peaks in the XRD patterns of SL-AgNPs and SS-AgNPs indicated that the AgNPs synthesized in the nano-regime have a crystalline nature.[30]

The size of the AgNPs was determined from the XRD pattern based on the line width of the peak with the highest intensity. The average crystal size (D) was calculated using the Scherrer equation:

$$D = (0.9\ \lambda)/(\beta \cos \theta)$$

where D represents the mean particle size, λ indicates the wavelength of the X-ray source, 2θ º is the Bragg's angle and β is the corrected Full Width at Half Maximum (FWHM) in radians. The average size of SL-AgNps and SS-AgNPs is approximately 11.85 nm and 14.82 nm, respectively. Similarly, the mean crystal size of AgNPs from *Perilla frutescens* was determined to be 15 nm.[31]

Scanning Electron Microscopy (SEM)

The morphology and size of green-synthesized SL-AgNPs and SS-AgNPs were studied using SEM. As observed in Figures (4a and 4b) nanoparticles predominantly exhibited spherical and ellipsoidal shapes, with irregular granulation and minimal aggregation. The aggregation of nanoparticles observed is likely due to solvent evaporation during sample preparation.[32,33] These results are consistent with previous studies.[18,31]

Fourier-Transformed Infrared spectroscopy (FT-IR)

FT-IR analysis was conducted to identify the potential biomolecules in the *Secamone emetica* leaf and stem extract. FT-IR spectra of leaf extract and synthesized SL-AgNPs are displayed in Figures (5a and 5b). In the leaf extract (Figure 5a), the most significant peaks were observed at 3353 cm^{-1}, 2928 cm^{-1}, 1718 cm^{-1}, 1606 cm^{-1}, 1516 cm^{-1}, 1452 cm^{-1}, 1381 cm^{-1}, 1277 cm^{-1}, 1165 cm^{-1}, 1122 cm^{-1}, 1065 cm^{-1}. For the SL-AgNPs (Figure 5b), prominent peaks were observed at 3357 cm^{-1}, 2924 cm^{-1}, 2858 cm^{-1}, 1720 cm^{-1}, 1632 cm^{-1}, 1452 cm^{-1}, 1381 cm^{-1}, 1261 cm^{-1}, 1045 cm^{-1}, respectively. Both the spectra showed similarities, in the leaf extract the band at 3353 cm^{-1}, assigned to OH stretching of alcohols and phenols,[34] shifted to 3357 cm^{-1} in the SL-AgNPs spectrum. These shifts may indicate small modifications in bond stretching or bending vibrations as the biomolecules adapt to their new role as capping agents, stabilizing the nanoparticles and preventing aggregation.[35] A shift is also observed for a peak at 2928 cm^{-1} dedicated to the OH stretch of phenolic compounds in leaf extract, moving to 2924 cm^{-1} in the SL-AgNPs band. The peak at 1380cm^{-1} corresponded to C-N stretching vibrations or O-H bending vibrations of both phenols or carboxylic acids,

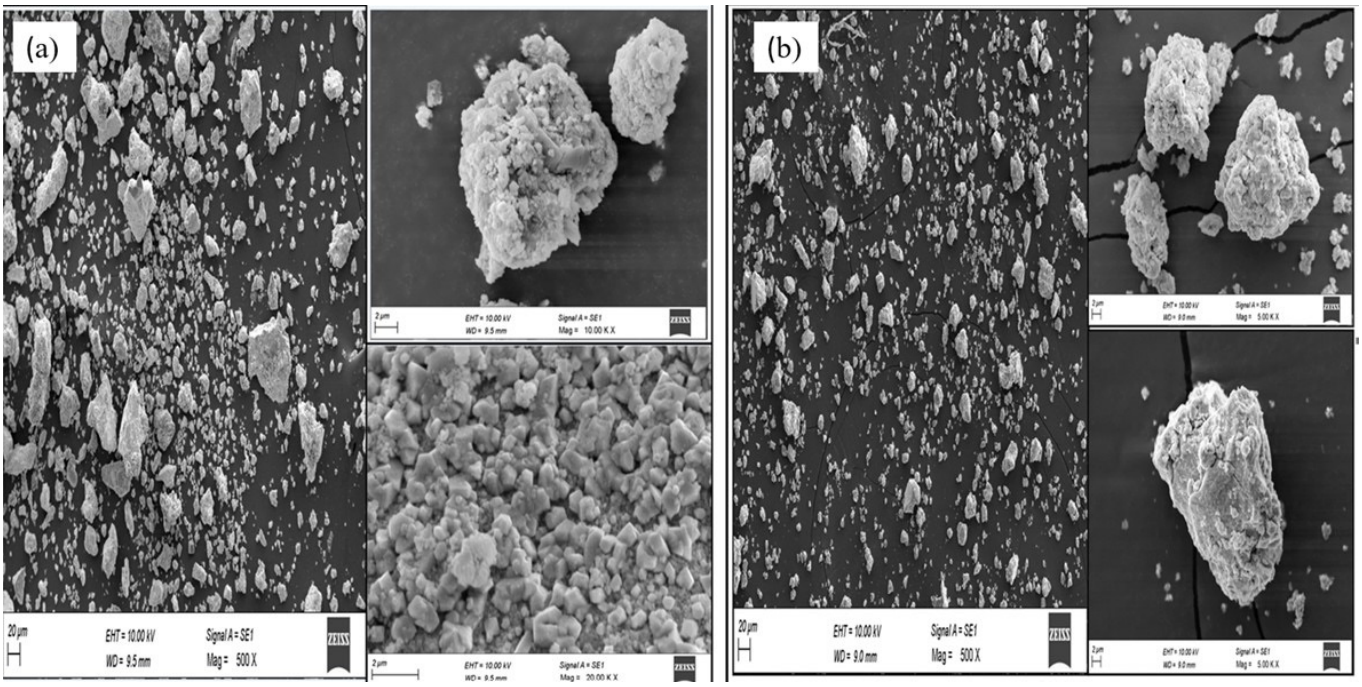

Figure 4: Scanning electron microscope (SEM) images of (a) SL-AgNPs and (b) SS-AgNPs.

which were observed in both spectra.[36] The stretching at 1122 cm^{-1} in plant extract specifies the occurrence of heterocyclic compounds, such as alkaloids and flavonoids.[37] The strong band at 1065 cm^{-1} in plant extract likely corresponding to the ether linkages of flavanones,[38] shifts to a lower frequency of 1045 cm^{-1} in the SL-AgNPs band, indicating C-O, alkene and other aliphatic stretching.[39]

In the stem extract (Figure 6a) the peaks observed at 3281 cm^{-1}, 2921 cm^{-1}, 1637 cm^{-1}, 1384 cm^{-1}, 1255 cm^{-1}, 1074 cm^{-1}, 1043 cm^{-1}. For the SS-AgNPs (Figure b), the peaks were observed at 3740 cm^{-1}, 3340 cm^{-1}, 2978 cm^{-1}, 2371 cm^{-1}, 1781 cm^{-1}, 1639 cm^{-1}, 1516 cm^{-1}, 1405 cm^{-1}, 1240 cm^{-1}, 1093 cm^{-1}, 914 cm^{-1}, 714 cm^{-1}. From the data. it is evident that both spectrums primarily show slight variations in the intensity of functional groups, indicating chemical changes that arose during the nanoparticle formation. The band at 3281 cm^{-1} in stem extract and 3740 cm^{-1} in the SS-AgNPs is assigned to the OH group,[40,41] representing polyphenols or alcohols. Literature indicates that phenolic acids serve as both reducing agents and stabilizers in the synthesis of nanoparticles.[42] C-H stretches were observed at 2921 cm^{-1} (in stem extract) and 2978 cm^{-1}(in SS-AgNPs) which represent alkanes or hydrocarbons.[43,44] The strong C-O stretches at 1255cm^{-1} and 1074cm^{-1} in the extract and 1240 cm^{-1} and 1093 cm^{-1} in the SS-AgNPs indicate the occurrence of alcohols, ethers or esters functional groups.[45,46] Alcohol, aldehydes, esters, lactones, ethers, ketones and phenol act as surface-active compounds to stabilize the nanoparticles.[47,48]

Biological Activity

Antioxidant assays

DPPH⁺ Radical Scavenging Assay

The capacity of the AgNPs produced via the aqueous extract of *Seacmone emetica* leaf and stem to reduce DPPH was measured spectrophotometrically at 517 nm. It was detected that the purple hue changed to a yellowish tint compared to the control. These color shifts may have resulted from the antioxidant's capacity to provide hydrogen.[23] The results indicate that both SL-AgNPs and SS-AgNPs exhibit antioxidant activity in dose-dependent manner Figure 7a.

At lower concentrations (10 and 20 µg/mL), SL-AgNPs surpassed the standard, showing 43.51% and 48.54% inhibition, respectively. However, at 100 µg/mL concentration, SL-AgNPs demonstrated 80.90% activity, which is similar to the standard ascorbic acid, which showed 89.23% inhibition. In comparison, SS-AgNPs showed substantial activity of 70.68% of maximum inhibition at 100 µg/mL concentration. In the parallel study, *Cleistanthus collinus* leaf-derived AgNPs exhibited a higher inhibition rate of 51.39% compared to the stem-derived AgNPs, which showed 49.94% at 500µg/m.[49] Similarly, a previous study noted 80%

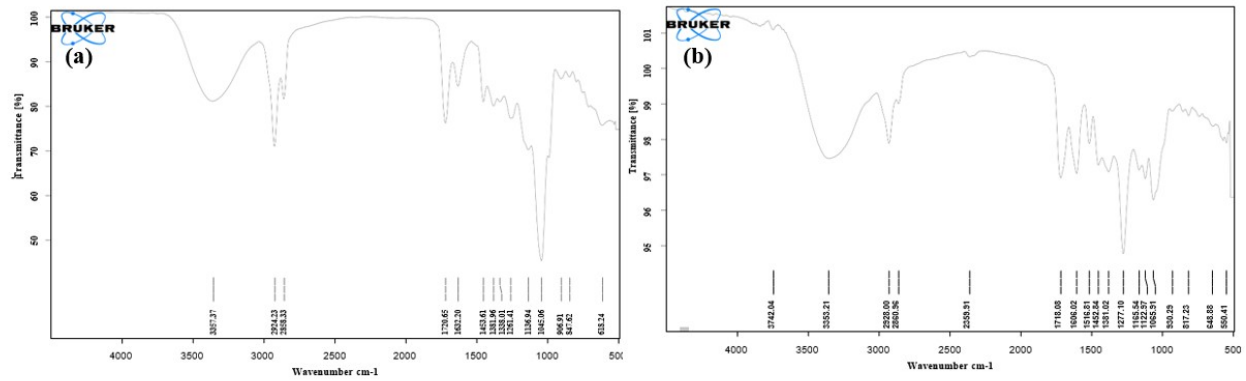

Figure 5: FTIR spectra of (a) *Secamone emetica* leaf extract and (b) SL-AgNPs.

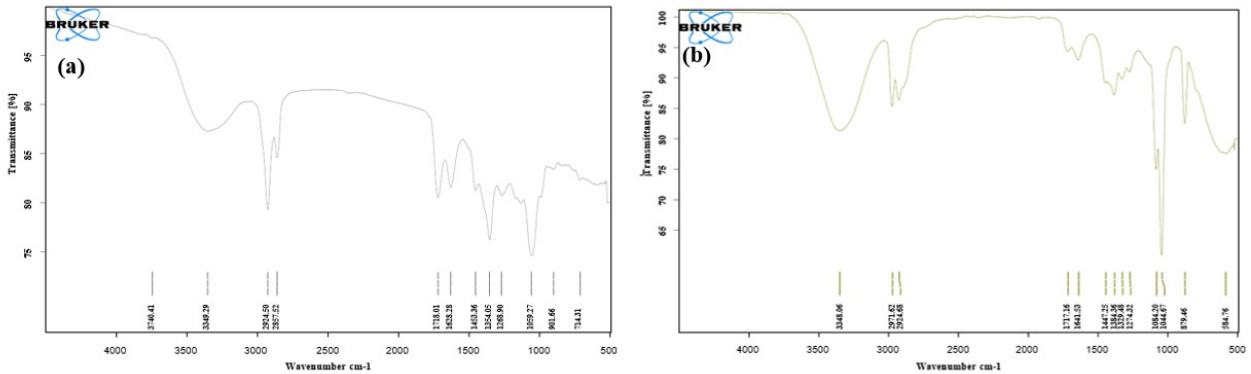

Figure 6: FTIR spectra of (a) *Secamone emetica* stem extract and (b) SS-AgNPs.

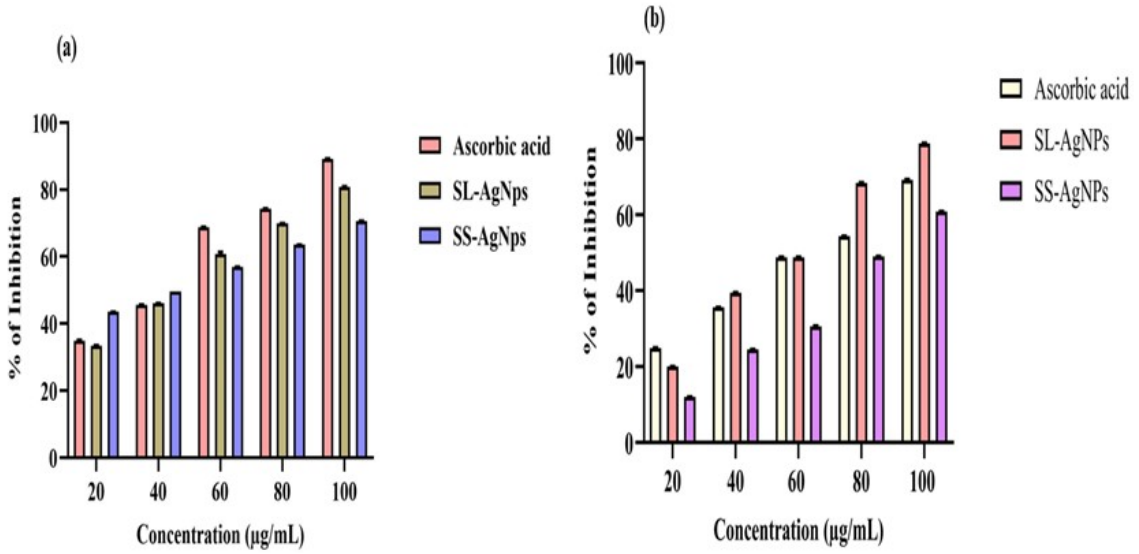

Figure 7: Antioxidant activity of SL-AgNPs and SS-AgNPs: (a) DPPH radical scavenging activity and (b) $ABTS^{\cdot}$+ scavenging activity.

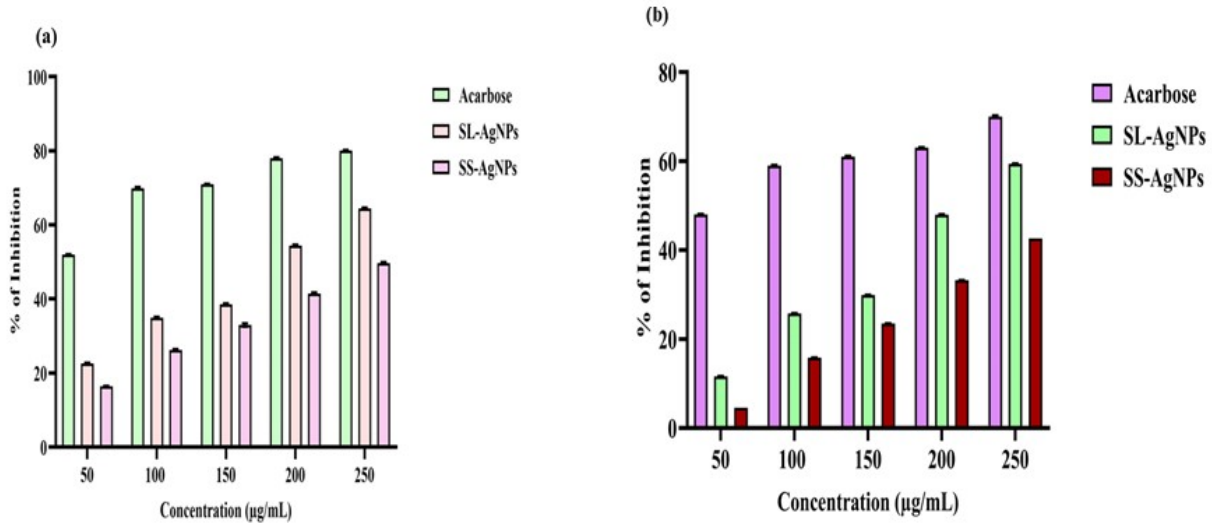

Figure 8: *In vitro* antidiabetic activity of SL-AgNPs and SS-AgNPs: (a) α-glucosidase assay and (b) α-amylase assay.

inhibition at 100 µg/mL for AgNPs synthesised from the leaf extract of *Crotonbon plandianum*.[50] The reaction of DPPH towards antioxidants occurs through electron transfer and hydrogen atom donor.[47] The synthesized AgNPs are expected to be abundant in hydrogen following the addition of the free radical (DPPH). Consequently, biosynthesised AgNPs hold potential as antioxidative agents.[51]

$ABTS^{\cdot+}$ Assay

The SL-AgNPs and SS-AgNPs demonstrated significant competence in ABTS radical scavenging activity in a dose-responsive manner (Figure 7b). At higher concentrations, SL-AgNPs consistently outperformed the standard (ascorbic acid) by exhibiting higher scavenging activity. Meanwhile, SS-AgNPs also showed considerable inhibition of 60.84% compared to the standard, which exhibited 69.23% inhibition at 100 µg/mL concentration. These findings were in line with earlier studies as the AgNPs produced from the leaf extract of *Asphodelus aestivus*'s demonstrated superior ABTS scavenging activity.[52] Similarly, at 100 µg mL, *Chenopodium garcini* leaf extract exhibits a noteworthy level of antioxidant activity.[53] In contrast, AgNPs made from *Ananas comosus* leaf extract demonstrated a moderate level of ABTS scavenging activity.[54]

In vitro Antidiabetic Activity

α-Amylase and α-glucosidase are crucial enzymes in carbohydrate metabolism.[55] Therefore, the anti-diabetic activity of SL-AgNPs and SS-AgNPs was assessed using *in vitro* α-amylase and α-glucosidase inhibition assays, as given in Figures (8a and 8b). Both SL-AgNPs and SS-AgNPs exhibited concentration-dependent suppression of α-amylase and α-glucosidase. At the maximum concentration of 250 µg/mL, SL-AgNPs showed 64.44% inhibition

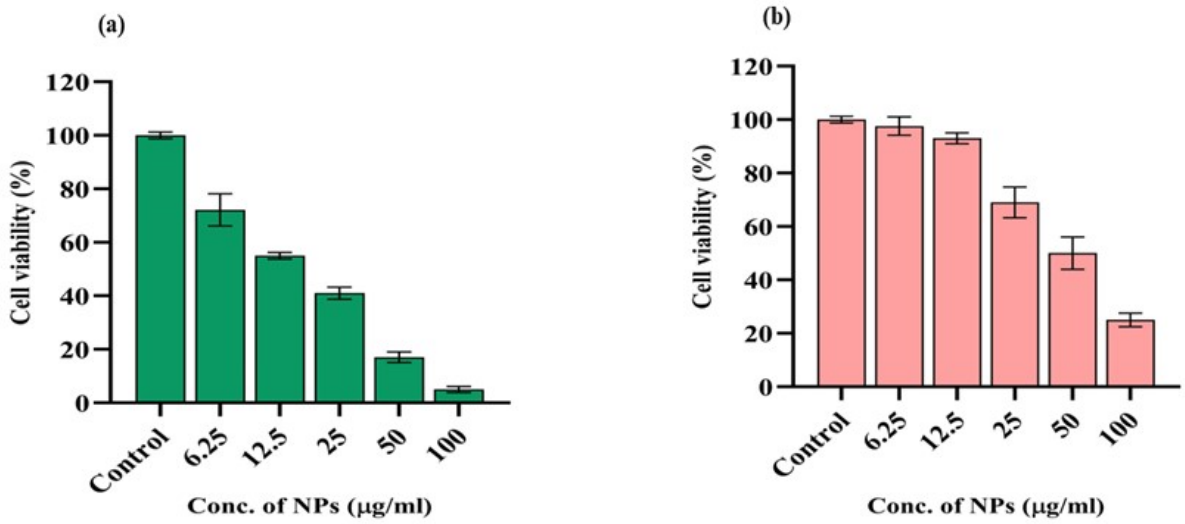

Figure 9: Effect of different concentrations of (a) SL-AgNPs and (b) SS-AgNPs on the viability of MCF-7 breast cancer cells.

in the α-glucosidase assay, while SS-AgNPs demonstrated 49.72% inhibition. In comparison, acarbose achieved 64.44% inhibition at the concentration. The IC_{50} value for acarbose was determined to be 36.70 µg/mL, whereas SL-AgNPs and SS-AgNPs showed IC_{50} values of 63.3 µg/mL and 86.04 µg/mL, respectively. Similarly, in the α-amylase assay, SL-AgNPs demonstrated 59.42% inhibition at 250 µg/mL, while SS-AgNPs exhibited 42.62% inhibition. In contrast, acarbose achieved 70% inhibition at the same concentration in the α-amylase assay. The IC_{50} values were 43.75 µg/mL for acarbose, 71.91 µg/mL for SL-AgNPs and 85 µg/mL for SS-AgNPs, indicating that leaf-derived nanoparticles had a stronger inhibitory effect compared to the stem-derived counterparts. Previously AgNPs from *Achillea maritima* confirmed high inhibition of α-amylase and α-glucosidase, with IC_{50} values of 64.9 and 41.6 g/mL, respectively. The literature contains several reports on the anti-diabetic efficacy of AgNPs from plant extracts.[56-58]

In vitro Anti-Cancer Activity

The MTT assay is a quantitative technique for evaluating cell viability and proliferation. In this experiment, MTT is cleaved by mitochondrial dehydrogenase in living cells, resulting in the formation of purple formazan crystals. The degree of cytotoxicity can be assessed by measuring the amount of formazan generated, which is directly correlated with the number of live cells.[59] The cytotoxic effect of the SL-AgNPs and SS-AgNPs in the breast cancer cell line (MCF-7) was assessed using an MTT assay. The experiment was performed using various concentrations of AgNPs (6.25, 12.5,25, 50 and 100 µg). The effect of the samples on cell viability is given in Figures (9a and 9b). The result specifies that the SL-AgNPs and SS-AgNPs induced cell death in a concentration-dependent fashion. Although both the samples showed promising cytotoxic activity, SL-AgNPs exhibited greater efficacy compared to SS-AgNPs. The IC_{50} values for SL-AgNPs and SS-AgNPs were 21.65 (µg/mL) and 50 (µg/mL), respectively.

The potent cytotoxic effect of leaf-derived AgNPs may be credited to the high content of bioactive metabolites, such as phenols and flavonoids. These bioactive compounds may cause cell mortality through various mechanisms, such as apoptosis, Reactive Oxygen Species (ROS) production and autophagy activation, all of which may contribute to their anti-neoplastic properties.[60] These results are corroborated by *in vitro* investigations showing that AgNPs can enter cells through endocytosis and cumulate in the endolysosomal compartment and the perinuclear area.[61]

Furthermore, AgNPs can penetrate mitochondria, triggering the generation of Reactive Oxygen Species (ROS) and altering cellular respiration. These reactive species contribute to the cytotoxic effects of AgNPs by indicating oxidative stress, apoptosis, DNA damage and mitochondrial dysfunction in cancer cells.[62] Thus, into their bioactive component, the increased cytotoxicity of SL-AgNPs may also be described by their capacity to generate ROS and indicate mitochondrial malfunction, disrupting critical cellular functions. Previously, AgNPs from *Perilla frutescens* showed moderate toxicity of 46.75% on MCF-7 breast cancer cell lines at a concentration 600 µg/mL.[31] Similarly, *Syzygium jambolanum* exhibited nanoparticles exhibited effective anti-cancerous activity, with an IC_{50} value of 2588 ppm/100 µL against the MCF-7 breast cancer cell line.[63]

CONCLUSION

In the current investigation, we carried out successful synthesis of AgNPs using reducing and capping biomolecules from the aqueous leaf and stem extract of *Secamone emetica*. The biosynthesis of SL-AgNPs and SS-AgNPs was verified using various techniques, including UV-visible spectroscopy, X-ray

diffraction, SEM and FTIR. Both SL-AgNPs and SS-AgNPs exhibited notable antioxidant activity in $DDPH^+$ and $ABTS^{\cdot+}$ assays. Additionally, *in vitro* antidiabetic assays highlight the therapeutic potential of SL-AgNPs and SS-AgNPs through α-amylase and α-glucosidase enzymes. The SL-AgNPs and SS-AgNPs also demonstrated promising cytotoxicity against MCF-7 breast cancer cells. This is report on the green synthesis of silver nanoparticles using Secamone emetica can inspire further extensive research into the therapeutic applications of these green-synthesized nanoparticles.

CONFLICT OF INTEREST

The authors declare that there is no conflict of interest.

FUNDING

No specific funding was received to conduct this research work.

ABBREVIATIONS

AgNPs: Silver Nanoparticles; **BSI:** Botanical Survey of India; **DMSO:** Dimethyl Sulfoxide; **DNS:** 3,5-Dinitrosalicylic Acid; **DMEM:** Dulbecco's Modified Eagle Medium; **DPPH:** 2,2-Diphenyl-1-Picrylhydrazyl; **FTIR:** Fourier Transform Infrared; **FBS:** Fetal Bovine Serum; **IC_{50}:** Inhibitory Concentration 50%; **mM:** Millimolar; **MTT:** 3-(4,5-Dimethylthiazol-2-yl)-2,5-Diphenyltetrazolium Bromide; **Na_2CO_3:** Sodium Carbonate; **NaOCl:** Sodium Hypochlorite; **pNPG:** p-Nitrophenyl Glucopyranoside; **rpm:** Revolutions per Minute; **RT:** Room Temperature; **SEM:** Scanning Electron Microscopy; **SPR:** Surface Plasmon Resonance; **XRD:** X-ray Diffraction.

SUMMARY

In this study, we successfully synthesized Silver Nanoparticles (AgNPs) using aqueous extracts of the Leaf (SL) and Stem (SS) of *Secamone emetica* through an eco-friendly green synthesis approach. The nanoparticles were characterized using UV-vis spectroscopy, X-ray diffraction (XRD), Fourier-Transform Infrared spectroscopy (FTIR) and Scanning Electron Microscopy (SEM), confirming their crystalline nature and the involvement of functional groups in the nanoparticle formation.

Biological evaluations demonstrated significant activities of the synthesized AgNPs. Antioxidant assays (DPPH+ and $ABTS^{\cdot}$+) revealed dose-dependent free radical scavenging properties, with SL-AgNPs showing superior performance compared to SS-AgNPs. In anti-diabetic assays, SL-AgNPs exhibited higher inhibitory effects on α-amylase and α-glucosidase, underscoring their potential in diabetes management. Cytotoxicity studies against MCF-7 breast cancer cells indicated dose-dependent cell viability reduction, with SL-AgNPs demonstrating greater potency than SS-AgNPs. This research highlights *Secamone emetica* as a valuable source for the green synthesis of AgNPs, offering significant antioxidant, anti-diabetic and anticancer properties. These findings lay a strong foundation for further investigation of *S. emetica*-derived nanoparticles in therapeutic applications.

REFERENCES

1. Singh R, Hano C, Nath G, Sharma B. Green Biosynthesis of Silver Nanoparticles Using Leaf Extract of *Carissa carandas* L. and Their Antioxidant and Antimicrobial Activity against Human Pathogenic Bacteria. Biomolecules. 2021;11(2):299. doi: 10.3390/biom11020299, PMID 33671333.
2. Abdellatif AA, Alhathloul SS, Aljohani AS, Maswadeh H, Abdallah EM, Hamid Musa KH, *et al.* Green synthesis of silver nanoparticles incorporated aromatherapies utilized for their antioxidant and antimicrobial activities against some clinical bacterial isolates. Bioinorg Chem Appl. 2022; 2022:2432758. doi: 10.1155/2022/2432758, PMID 35449714.
3. Alwhibi MS, Soliman DA, Awad MA, Alangery AB, Al Dehaish H, Alwasel YA. Green synthesis of silver nanoparticles: characterization and its potential biomedical applications. Green Process Synth. 2021;10(1):412-20. doi: 10.1515/gps-2021-0039.
4. Abd El-Moaty HI, Soliman NA, Hamad RS, Ismail EH, Sabry DY, Khalil MM. Comparative therapeutic effects of *Pituranthos tortuosus* aqueous extract and phyto-synthesized gold nanoparticles on Helicobacter pylori, diabetic and cancer proliferation. S Afr J Bot. 2021;139:167-74. doi: 10.1016/j.sajb.2021.02.009.
5. Chandraker SK, Ghosh MK, Lal M, Shukla R. A review on plant-mediated synthesis of silver nanoparticles, their characterization and applications. Nano Express. 2021;2(2). doi: 10.1088/2632-959X/ac0355.
6. Ibrahim HM. Green synthesis and characterization of silver nanoparticles using banana peel extract and their antimicrobial activity against representative microorganisms. J Radiat Res Appl Sci. 2015;8(3):265-75. doi: 10.1016/j.jrras.2015.01.007.
7. Aiyambo D. Traditional uses of selected members of the *Apocynaceae* family in Namibia. Ministry of agriculture. Windhoek: Water and Forestry; 2010.
8. Bhadane BS, Patil MP, Maheshwari VL, Patil RH. Ethnopharmacology, phytochemistry and biotechnological advances of family *Apocynaceae*: a review. Phytother Res. 2018;32(7):1181-210. doi: 10.1002/ptr.6066, PMID 29575195.
9. Karuppusamy S. Medicinal plants used by Paliyan tribes of Sirumalai hills of Southern India. Nat Prod Radiance. 2007;6(5):436-42.
10. S S, N S, R J, Dh G. Morpho-anatomical studies on *Secamone emetica* (Retz.) R. Br. ex Sm.-an endemic medicinal plant. Pharmacogn Res. 2024;16(2):275-81. doi: 10.5530/pres.16.2.35.
11. Vaiyapuri M, Raju K, Karuppusamy S. Preliminary phytochemical investigation on *Secamone emetica* (Retz.) R. Br. (*Apocynaceae*)-an endemic medicinal plant species of Southern India. J Pharmacogn Phytochem. 2015;3(6).
12. Sekar T, Francis K. Some plant species screened for energy, hydrocarbons and phytochemicals. Bioresour Technol. 1998;65(3):257-9. doi: 10.1016/S0960-8524(98)00029-7.
13. Sini KR, Sinha BN, Karpagavalli M. Determining the antioxidant activity of certain medicinal plants of Attapady, (Palakkad), India using DPPH assay. Curr Bot. 2010;1(1):13-6.
14. Harborne JB. Phytochemical methods. 3rd ed. Springer (India) Private Limited; 1998.
15. Evans WC. Trease and Evans' pharmacognosy. 14th ed. W. B. Saunders Company Limited; 2000.
16. Kokate CK, Purohit AP, Gokhale SB. Textbook of pharmacognosy. 27th ed Nirali Prakashan; 2004.
17. Khandelwal KR. Practical pharmacognosy. 19th ed Nirali Prakashan; 2008.
18. Hemlata P, Meena PR, Singh AP, Tejavath KK. Biosynthesis of silver nanoparticles using *Cucumis prophetarum* aqueous leaf extract and their antibacterial and antiproliferative activity against cancer cell lines. ACS Omega. 2020;5(10):5520-8. doi: 10.1021/acsomega.0c00155, PMID 32201844.
19. Miller GL. Use of dinitrosalicylic acid reagent for determination of reducing sugar. Anal Chem. 1959;31(3):426-8. doi: 10.1021/ac60147a030.
20. Alley MC, Scudiere DA, Monks A, Czerwinski M, Shoemaker II R, Boyd MR. Validation of an automated microculture tetrazolium assay (MTA) to assess growth and drug sensitivity of human tumor cell lines. Proc Am Assoc Cancer Res. 1986;27:389.
21. Mosmann T. Rapid colorimetric assay for cellular growth and survival: application to proliferation and cytotoxicity assays. J Immunol Methods. 1983;65(1-2):55-63. doi: 10.1016/0022-1759(83)90303-4, PMID 6606682.
22. Jha AK, Prasad K, Prasad K, Kulkarni AR. Plant system: Nature's nano factory. Colloids Surf B Biointerfaces. 2009;73(2):219-23. doi: 10.1016/j.colsurfb.2009.05.018, PMID 19539452.
23. Narayanan M, Divya S, Natarajan D, Senthil-Nathan S, Kandasamy S, Chinnathambi A, *et al.* Green synthesis of silver nanoparticles from aqueous extract of *Ctenolepis garcini* L. and assess their possible biological applications. Process Biochem. 2021;107:91-9. doi: 10.1016/j.procbio.2021.05.008.
24. Bilal M, Rasheed T, Iqbal HM, Li C, Hu H, Zhang X. Development of silver nanoparticles loaded chitosan-alginate constructs with biomedical potentialities. Int J Biol Macromol. 2017;105(1):393-400. doi: 10.1016/j.ijbiomac.2017.07.047, PMID 28705499.

25. Bahuguna G, Kumar A, Mishra NK, Kumar C, Bahlwal A, Chaudhary P, *et al.* Green synthesis and characterization of silver nanoparticles using aqueous petal extract of the medicinal plant Combretum indicum. Mater Res Express. 2016;3(7):075003. doi: 10.1088/2053-1591/3/7/075003.
26. Vijayaraghavan K, Nalini SP, Prakash NU, Madhankumar D. One-step green synthesis of silver nano/microparticles using extracts of *Trachyspermum ammi* and *Papaver somniferum*. Colloids Surf B Biointerfaces. 2012;94:114-7. doi: 10.1016/j.colsurfb.2012.01.026, PMID 22348989.
27. Alaraidh IA, Ibrahim MM, El-Gaaly GA. Evaluation of green synthesis of Ag nanoparticles using *Eruca sativa* and *Spinacia oleracea* leaf extracts and their antimicrobial activity. Iran J Biotechnol. 2014;12(1):50-5. doi: 10.5812/ijb.12392.
28. Sathyavathi R, Krishna MB, Rao SV, Saritha R, Rao DN. Biosynthesis of silver nanoparticles using *Coriandrum sativum* leaf extract and their application in nonlinear optics. Adv Sci Lett. 2010;3(2):138-43. doi: 10.1166/asl.2010.1099.
29. Ponarulselvam S, Panneerselvam C, Murugan K, Aarthi N, Kalimuthu K, Thangamani S. Synthesis of silver nanoparticles using leaves of *Catharanthus roseus* Linn. G. Don and their antiplasmodial activities. Asian Pac J Trop Biomed. 2012;2(7):574-80. doi: 10.1016/S2221-1691(12)60100-2, PMID 23569974.
30. Swamy MK, Akhtar MS, Mohanty SK, Sinniah UR. Synthesis and characterization of silver nanoparticles using fruit extract of *Momordica cymbalaria* and assessment of their *in vitro* antimicrobial, antioxidant and cytotoxicity activities. Spectrochim Acta A Mol Biomol Spectrosc. 2015;151:939-44. doi: 10.1016/j.saa.2015.07.009, PMID 26186612.
31. Tavan M, Hanachi P, Mirjalili MH, Dashtbani-Roozbehani A. Comparative assessment of the biological activity of the green synthesized silver nanoparticles and aqueous leaf extract of *Perilla frutescens* (L.). Sci Rep. 2023;13(1):6391. doi: 10.1038/s41598-023-33625-x, PMID 37076588.
32. Vijay Kumar PP, Pammi SV, Kollu P, Satyanarayana KV, Shameem U. Green synthesis and characterization of silver nanoparticles using *Boerhaavia diffusa* plant extract and their antibacterial activity. Ind Crops Prod. 2014;52:562-6. doi: 10.1016/j.indcrop.2013.10.050.
33. Sigamoney M, Shaik S, Govender P, Krishna SB, Sershen. African leafy vegetables as bio-factories for silver nanoparticles: A case study on *Amaranthus dubius* C Mart. ex Thell. S Afr J Bot. 2016;103:230-40. doi: 10.1016/j.sajb.2015.08.022.
34. Khan MZ, Tareq FK, Hossen MA, Roki MN. Green synthesis and characterization of silver nanoparticles using *Coriandrum sativum* leaf extract. J Eng Sci Technol. 2018;13(1):158-66.
35. Rathi PR, Reka M, Poovazhagi R, Arul Kumar M, Murugesan K. Antibacterial and cytotoxic effect of biologically synthesized silver nanoparticles using aqueous root extract of *Erythrina indica* Lam. Spectrochim Acta A Mol Biomol Spectrosc. 2015;135:1137-44. doi: 10.1016/j.saa.2014.08.019, PMID 25189525.
36. Khan M, Karuppiah P, Alkhathlan HZ, Kuniyil M, Khan M, Adil SF, *et al.* Green synthesis of silver nanoparticles using *Juniperus procera* extract: their characterization and biological activity. Crystals. 2022;12(3). doi: 10.3390/cryst12030420.
37. Jayaprakash N, Judith Vijaya J, John Kennedy L, Priadharsini K, Palani P. One-step phytosynthesis of highly stabilized silver nanoparticles using *Piper nigrum* extract and their antibacterial activity. Mater Lett. 2014;137:358-61. doi: 10.1016/j.matlet.2014.09.027.
38. Shankar SS, Rai A, Ahmad A, Sastry M. Rapid synthesis of Au, Ag and bimetallic au core-Ag shell nanoparticles using Neem (*Azadirachta indica*) leaf broth. J Colloid Interface Sci. 2004;275(2):496-502. doi: 10.1016/j.jcis.2004.03.003, PMID 15178278.
39. Kalyanasundaram N, Sivakumar N, Devendrapandi G, Selvakumar P. Black *Datura fastuosa* flower extract-mediated green synthesis of silver nanoparticles and their antibacterial activity. Int J Sci Technol Res. 2020;9(2).
40. Imuetinyan H, Junin R. Analysis of crude saponin from the leaves of *Vernonia amygdalina*. Int J Sci Res Chem. 2019;4(6):1-4.
41. Fabiani VA, Sari FI, Nur'aini SA, Putri SA. Biosynthesis and characterization of zinc ferrite (ZnFe2O4) via *Antidesma bunius* L. fruit extract. IOP Conf Ser Earth Environ Sci. 2021;926(1):012061. doi: 10.1088/1755-1315/926/1/012061.
42. Amini SM, Akbari A. Metal nanoparticles synthesis through natural phenolic acids. IET Nanobiotechnol. 2019;13(8):771-7. doi: 10.1049/iet-nbt.2018.5386, PMID 31625516.
43. Prathyusha S. Formulation, phytochemical and antioxidant activity evaluation of selected Indian medicinal plants. Ann Phytomed. 2022; 11(Special Issue 1). doi: 10.54085/ap.trips.2022.11.1.7.
44. Arunprasath A, Indhumathi M. Identification of functional groups in Corbichonia decumbens by Fourier-transform infrared spectroscopy. J Drug Deliv Ther. 2019;9(3-s):583-7. doi: 10.22270/jddt.v9i3-s.3003.
45. Zhang YC, Deng J, Lin XL, Li YM, Sheng HX, Xia BH, *et al.* Use of ATR-FTIR spectroscopy and chemometrics for the variation of active components in different harvesting periods of Lonicera japonica. Int J Anal Chem. 2022;2022(1):8850914. doi: 10.1155/2022/8850914, PMID 35295923.
46. Bensemmane N, Bouzidi N, Daghbouche Y, Garrigues S, de la Guardia M, El Hattab M. Quantification of phenolic acids by partial least squares Fourier-transform infrared (PLS-FTIR) in extracts of medicinal plants. Phytochem Anal. 2021;32(2):206-21. doi: 10.1002/pca.2974, PMID 32666562.
47. Wang Y, Li Q, Peng X, Li Z, Xiang J, Chen Y, *et al.* Green synthesis of silver nanoparticles through oil: promoting full-thickness cutaneous wound healing in methicillin-resistant *Staphylococcus aureus* infections. Front Bioeng Biotechnol. 2022;10:856651. doi: 10.3389/fbioe.2022.856651, PMID 36082170.
48. Song JY, Kim BS. Rapid biological synthesis of silver nanoparticles using plant leaf extracts. Bioprocess Biosyst Eng. 2009;32(1):79-84. doi: 10.1007/s00449-008-0224-6, PMID 18438688.
49. Chiu HI, Che Mood CN, Mohamad Zain NN, Ramachandran MR, Yahaya N, Nik Mohamed Kamal NN, *et al.* Biogenic silver nanoparticles of *Clinacanthus nutans* as antioxidant with antimicrobial and cytotoxic effects. Bioinorg Chem Appl. 2021;2021:9920890. doi: 10.1155/2021/9920890, PMID 34093698.
50. Kumar V, Mohan S, Singh DK, Verma DK, Singh VK, Hasan SH. Photo-mediated optimized synthesis of silver nanoparticles for the selective detection of iron(III), antibacterial and antioxidant activity. Mater Sci Eng C Mater Biol Appl. 2017;71:1004-19. doi: 10.1016/j.msec.2016.11.013, PMID 27987654.
51. Huang D, Ou B, Prior RL. The chemistry behind antioxidant capacity assays. J Agric Food Chem. 2005;53(6):1841-56. doi: 10.1021/jf030723c, PMID 15769103.
52. Fafal T, Taştan P, Tüzün BS, Ozyazici M, Kivcak B. Synthesis, characterization and studies on antioxidant activity of silver nanoparticles using *Asphodelus aestivus* Brot. aerial part extract. S Afr J Bot. 2017;112:346-53. doi: 10.1016/j.sajb.2017.06.019.
53. Abdel-Aziz MS, Shaheen MS, El-Nekeety AA, Abdel-Wahhab MA. Antioxidant and antibacterial activity of silver nanoparticles biosynthesized using *Chenopodium murale* leaf extract. J Saudi Chem Soc. 2014;18(4):356-63. doi: 10.1016/j.jscs.2013.09.011.
54. Das G, Patra JK, Debnath T, Ansari A, Shin HS. Investigation of antioxidant, antibacterial, antidiabetic and cytotoxicity potential of silver nanoparticles synthesized using the outer peel extract of *Ananas comosus* (L.). PLOS One. 2019;14(8):e0220950. doi: 10.1371/journal.pone.0220950, PMID 31404086.
55. Ahmed S, Ali MC, Ruma RA, Mahmud S, Paul GK, Saleh MA, *et al.* Molecular docking and dynamics simulation of natural compounds from betel leaves (*Piper betle* L.) for investigating the potential inhibition of alpha-amylase and alpha-glucosidase of type 2 diabetes. Molecules. 2022;27(14):4526. doi: 10.3390/molecules27144526, PMID 35889399.
56. Shanker K, Mohan GK, Hussain MA, Jayarambabu N, Pravallika PL. Green biosynthesis, characterization, *in vitro* antidiabetic activity and investigational acute toxicity studies of some herbal-mediated silver nanoparticles on animal models. Pharmacogn Mag. 2017;13(49):188-92. doi: 10.4103/0973-1296.197642, PMID 28216905.
57. Prabhu S, Vinodhini S, Elanchezhiyan C, Rajeswari D. Evaluation of antidiabetic activity of biologically synthesized silver nanoparticles using *Pouteria sapota* in streptozotocin-induced diabetic rats. J Diabetes. 2018;10(1):28-42. doi: 10.1111/1753-0407.12554, PMID 28323393.
58. Saratale RG, Shin HS, Kumar G, Benelli G, Kim DS, Saratale GD. Exploiting antidiabetic activity of silver nanoparticles synthesized using *Punica granatum* leaves and anticancer potential against human liver cancer cells (HepG2). Artif Cells Nanomed Biotechnol. 2018;46(1):211-22. doi: 10.1080/21691401.2017.1337031, PMID 28612655.
59. Prajapati C, Reddy M, Bhatt M. Evaluation of anticancer activity using leaf extract of *Simarouba glauca* on leukemic cancer cell lines. Int J Bot Stud. 2018;3(2):52-6.
60. Suseela V, Nirmaladevi R, Pallikondaperumal M, Priya RS, Shaik MR, Shaik AH, *et al.* Eco-friendly preparation of silver nanoparticles and their antiproliferative and apoptosis-inducing ability against lung cancer. Life (Basel). 2022;12(12):2123. doi: 10.3390/life12122123, PMID 36556488.
61. Greulich C, Diendorf J, Simon T, Eggeler G, Epple M, Köller M. Uptake and intracellular distribution of silver nanoparticles in human mesenchymal stem cells. Acta Biomater. 2011;7(1):347-54. doi: 10.1016/j.actbio.2010.08.003, PMID 20709196.
62. Kim S, Choi JE, Choi J, Chung KH, Park K, Yi J, *et al.* Oxidative stress-dependent toxicity of silver nanoparticles in human hepatoma cells. Toxicol *In Vitro*. 2009;23(6):1076-84. doi: 10.1016/j.tiv.2009.06.001, PMID 19508889.
63. Madakka M, Jayaraju N, Rajesh N. Evaluating the antimicrobial activity and antitumor screening of green synthesized silver nanoparticles compounds, using *Syzygium jambolanum*, towards MCF-7 cell line (Breast cancer cell line). J Photochem Photobiol. 2021;6:100028. doi: 10.1016/j.jpap.2021.100028.

Cite this article: Shalini S, Sudeepthi N, Geetha DH, Jayashre R. Green Synthesis of Silver Nanoparticles from *Secamone emetica*: Characterization and Assessment of Antioxidant, Anti-Diabetic and Anti-Cancer Activities against MCF-7 Breast Cancer Cells. Pharmacog Res. 2025;17(2):x-x.